MODELLING SENSIBLE HEAT FLUX IN MOUNTAINOUS AREAS WITH HIGH RESOLUTION TERRAIN PARAMETERS DERIVED FROM LANDSAT-TM DATA

Dipl. Geogr./Hydol. Jürgen Storl
President GEOTEC S.R.L.
Av. 20 de Octubre 2252 - La Paz - Bolivia
Fax: (591) (2) 37 49 97 - E-mail: geo@geo.bo

Commission VII, Working Group 5

KEY WORDS: Sensible heat flux, Remote sensing, Modelling, Energy budget, Soil moisture, Evapotranspiration

ABSTRACT

This article presents a method to model sensible heat flux on micro scale over mountainous terrain and shows how the model parameters can be derived at high resolution (30m) from Landsat-TM data, a digital terrain model and point measurements of atmospheric parameters.
Thermal information of Landsat channel 6 is transformed to a resolution of 30m, applying a multiple linear regression model that contains soil moisture information.
The modelling of sensible heat flux is performed using a slope wind model developed by Brehm (Brehm, 1986) and applied with NOAA AVHRR data by Mannstein (Mannstein, 1991) over the Alpes.
The modelling of sensible heat flux is placed in the context of an inventory of all energy budget terms.

1. INTRODUCTION

The local dynamics of heat interchange are subject to investigation in order to increase our understanding of micrometeorological processes.
Calculating senible heat flux on micro scale makes it possible to predict microclimatic changes due to changes in vegetation cover (Parlow, 1988, 1990).
Moreover, sensible heat flux is a highly usefull term to be calculated in order to derive actual evapotranspiration, the most difficult term of the energy budget to be modeled directly, due to its dependance on physiologic control by plants.
Understanding evapotranspiration, in turn, leads to an understanding of the water cycle for hydrologic and agricultural purposes.

The modelling of sensible heat flux with remotely sensed data is subject to many investigations, and a considerable number of methods have been developed for flat and uniform terrain, especially for certain crop types.
Few investigators have undertaken the task of modelling sensible heat flux from remotely sensed data over mountainous and highly inhomogeneous terrain, as it is presented in this study.

2. CONTEXT

The author developed a method applied by Mannstein (Mannstein, 1991) for modelling sensible heat flux over mountainous terrain. All model parameters were procesed at a resolution that allows the calculation of sensible heat flux on micro scale. The availability of a great amount of datasets for the study area made it possible to place the sensible heat flux modelling into the context of an energy budget integration. Therefore, a valuable instrument for verification was at hand.

3. DATA

The data used in the present study consisted of a satellite scene Landsat-TM, aquired on july 20, 1986 at 9h20 over the study area in northern scandinavia. All channels were radiation corrected using the short wave insulation model SWIM (Parlow, 1988, 1990, 1992, Parlow/Scherer 1991), and a detailed land use classification derived by Parlow (Parlow, 1988) from radiation corrected data was available.
Furthermore, the author could dispose of a PAR-albedo image (Albedo for Photosynthetically Active Radiation, Parlow, 1988, 1990), an image of solar irradiation calculated with the program SWIM (**S**hort **W**ave **I**nsulation **M**odel, University of Basel) and calibrated by Parlow and an image of longwave atmospheric counter radiation (Parlow, 1988).
For each land use class, detailed radiometric measurements of integral albedo had been performed by Parlow (Parlow, 1988, 1990, 1991) and were available to the author.
Thermal channel 6 of Landsat-TM had been calibrated by Parlow to radiance surface temperatures over the sea surface of lake Abisko, using a calibration formula suggested by Schott and Volchok (Schott/Volchok, 1985). The atmospheric influence was eliminated using an improved version of the WINDOW model of J. Price, NASA (WINDHA, Price, 1987 / ATMKOR, Scherer, 1987).
At the day of satellite overpass, all meteorological parameters of Abisko Station, inside the study area, were available, together with a collection of meteorological data from several years for the same station. A profile of air temperature, air- and vapour pressure had been taken by a radio sonde at Kallax/Lulea at the day of satellite overpass at 12h00 local time.

4. STUDY AREA

The Abisko National Park is situated in northern Sweden in the province Lappland at 6821'N/1999'E. The study area in the sub province Torne Lappmark includes the northern part of the Abisko National Park, part of lake Abisko, the hills south of Abisko Östra and the crests of mount Njulla (1169m) and Slattatjakka (1191m). In Scandinavia the northern limit of boreal forest is formed by the birch. The forest limit in the study area is determined by elevation and situated between 550m and 650m. It can be differentiated between the "subalpine birch tree region" and the "alpine region" of alpine heaths, meadows and tundra.

5. THE SLOPE WIND MODEL OF BREHM

Under stable conditions, the atmospheric boundary layer shows special characteristics at slopes, and a sun driven mecanism forces the air into a well defined movement upwards.

Brehm (Brehm, 1986) parametrized the slope wind by atmospheric stability, excess temperature (temperature difference between the terrain at roughness length-height and free atmosphere) and slope angle.

His model generates values for the geostrophic friction coefficient c_g, the heat transfer coefficient c_h and their ratio $\eta = c_g/c_h$, which are defined by the following equations:

$$c_g = \frac{u}{\kappa \Delta \sqrt{\beta/\gamma}} \quad (1)$$

$$\eta = \frac{\kappa\, u^* \Theta^* \sqrt{\beta/\gamma}}{u^{*2}} \quad (2)$$

Where u* is the friction velocity, Θ^* the characteristic temperature fluctuation, κ Von Karman's constant, Δ the excess temperature, β the coefficient between the acceleration due to gravity and the potential temperature of the surface g/Θ_o and the temperature gradient of the free atmosphere $d\Theta/dz$.

BREHM generated values for c_g and η in dependance of the analog soil rosby number Ro for different slope angles. Soil rosby number in turn is defined as follows:

$$Ro = \frac{\kappa \Delta}{\gamma \sin\alpha\, z_o} \quad (3)$$

z_o is the roughness length.
In order to calulate the analog soil rosby number for each terrain pixel, we need the surface temperature, a vertical temperature profile of the free atmosphere, a method to parametrize roughness length and a digital terrain for slope angles and elevations.
The relations between rosby number and c_g or η, calculated by Brehm's slope wind model, are graphically represented in Brehm's study (Brehm, 1986) in two graphics for different slope angles. The functional dependance between c_g / η and the rosby number for any slope angle were fitted by a polynomial equation, so that c_g and η could be written as functions $c_g = f(\alpha,Ro)$ and $\eta = f(\alpha,Ro)$.

6. PARAMETRIZATION OF SENSIBLE HEAT FLUX

Sensible heat flux can be written as follows:

$$H = -\rho\, c_p\, \kappa\, u^*\, \Theta^* \quad (4)$$

where ρ is the air density and c_p is the specific heat of air at constant pressure.

Replacing the parameters with de definitions of c_g and η in formula (1) and (2), equation (4) can be reformulated in the following way:

$$H = \rho\, c_p\, \kappa^2 c_g^2(Ro,\alpha)\, \eta(Ro,\alpha)\, \Delta^2 \sqrt{\beta/\gamma} \quad (5)$$

The excess temperature as formulated by Brehm is the temperature difference between the free atmosphere and the surface defined at a level above the ground that corresponds to roughness length.
Mannstein (Mannstein, 1991) assumes, that the radiation temperature derived from thermal sensors of a remote sensing devices represent the skin temperature of the ground which is best represented at zero height. Therefore, he adopts a formulation of Monin and Zilitinkevich (Monin/Zilitinkevich, 1968) which expresses the difference Δ_d between surface and z_o-level as follows:

$$\Delta_d = -0.13\, \Theta^* \left(\frac{u^*\, z_o}{\nu}\right)^{0.45} \quad (6)$$

ν is the kinematic viscosity of air.

Using the definitions for c_g and η, Δ_d can be written as:

$$\Delta_d = -0.13\, \kappa\, \eta\, c_g\, \Delta \left(\frac{c_g\, \kappa\, \Delta \sqrt{\beta/\gamma}\, z_o}{\nu}\right)^{0.45} \quad (7)$$

For a given temperature difference Δ_s between the ground (derived by thermal sensors) and free atmosphere, the temperature difference Δ between the z_o level and the atmosphere, as it will be used for the model, can be found by itereation, so that the following equation holds:

$$\Delta_s = \Delta + \Delta_d \quad (8)$$

Δs is the known temperature difference between satellite temperature at n=0 and free atmosphere.

7. DETERMINATION OF THE MODEL PARAMETERS

7.1 Modelling of roughness length

Roughness length varies widly within a given land use class. Mannstein distinguished only 3 land use types and substituted each of them with a single value for roughness length.

In this study, a highly differenciated land use classification had been calculated with radiation corrected data (Parlow, 1988, 1991, 1992) and was found to be coherent with the field mapping realized by the author (Storl, 1992).
For a modelling of sensible heat flux on micro scale, the intraclass variance of roughness length has to be taken into account and must be adecuately parametrized.
The author could dispose of a PAR-albedo dataset (**P**hotosynthetically **A**ctive **R**adiation albedo). PAR-albedo is the albedo for radiation in the photosynthetically active region of the spectra, and therefore an excellent biomass parameter that reflects vegetation density much better than NDVI, as has been shown by Parlow (Parlow, 1988).

In can be assumed, that PAR-albedo is correlated to stand height within a certain vegetation class, as absorption of photosynthetically active radiation is related to biomass, and more biomass means higher plants within one vegetation class in general.
As a first approximation, a linear relation was assumed between plant height and PAR-albedo within the classes.

In order to obtain a roughness length value for each 30x30m pixel, the information about intraclass variance variation inherent in the PAR-albedo dataset was integrated with the land use classification.
An image processing procedure (CSCALE, Storl, 1992, 1993, 1994) was written in order to scale each value of PAR-albedo according to its land use class. Therefore, representative values for roughness length and its standard deviation for each vegetation class were taken from the data accumulated at the Royal Academy of Science in Abisko.

Tab.1 shows the medium values and standard deviation of roughness length used in meters.

very dry heath	**dry heath**	**moist heath**	**meadow**	**snow**	**swamp**	**salix**
0,010	0,010	0,020	0,008	0,001	0,010	0,040
0,005	0,005	0,005	0,002	0,000	0,000	0,020
old birch forest	**heath birch forest**	**moist heath birch forest**	**constr.**	**water**		
0,500	0,400	0,600	0,900	0,001		
0,200	0,200	0,200	0,000	0,000		

Tab. 1. Mean roughness length and standard deviation for the land use classes

Conditioned scaling was applied to the PAR-albedo dataset, with the land use classes as conditioning parameters. For each land use class, CSCALE calculated the medium value and the standard deviation of PAR-albedo. In a second pass through the images, CSCALE transformed the PAR-albdo values in a linear way accordingly, assigning pixels with mean PAR-albedo value for the respective land use class the mean roughness length of the class, and transforming PAR-albedo values that varied about standard deviation from the mean values into roughness length values within the roughness lenth statistics of the respective class.

7.2 Surface temperature

The thermal channel 6 of Landsat TM with a spatial resolution of 120m had been calibrated by Parlow (Parlow, 1988) to radiance surface temperature over the sea surface of lake Abisko using a calibration formula suggested by Schott and Volchok (Schott/Volchok, 1985). The atmospheric influence was eliminated using an improved version of the WINDOW model of J. Price, NASA (WINDHA, Price, 1987 / ATMKOR, Scherer, 1987)

7.2.1 Resolution enhancement

The channels 1-5 and 7 of Landsat-TM have a spatial resolution of 30x30m, whereas the thermal channel 6 is restricted to a resolution of 120x120m.
Scherer (Scherer, 1987) developed a method to improve the spatial resolution of thermal data, integrating data sets of higher resolution. He obtained an enhanced spatial resolution of remotely sensed thermal data, using a multiple linear regression model, which he derived from the energy budget equation. The energy budget equation under equilibrium conditions can be written as:

$$E_{s\downarrow}(1-\alpha) + E_{l\downarrow} - E_{l\uparrow} + G + H + LE = 0 \qquad (9)$$

α ... integral albedo
Es ... short wave solar irradiation
E_l ... long wave atmospheric counter irradiation
E_l ... long wave terrestrial radiation
G ... soil heat flux
H ... sensible heat flux
LE ... latent heat flux (evapotranspiration)

Scherer showed, that equation (9) can be transformed with permissible approximations, representing long wave radiation as a linear combination of short wave irradiation, terrain elevation and the percentage of different land use classes in a pixel. He assumed a constant ratio between sensible and latent heat flux (Bowen Ratio) within each class. Hence, for each 120x120m thermal pixel of Landsat-TM, the following equation can be written (Scherer, 1987):

$$E_{l\uparrow} = a\,E_{s\downarrow} + b\,h + \sum_{i=1}^{n} c_i p_i + d \qquad (10)$$

Es ... short wave solar irradiation
h ... terrain elevation

p_i ... percentage of land use class i in the pixel
d ... regression constant, containing all factors not considered by the other parameters, like changing Bowen Ratio within land use classes.

The right side of the equation consists of parameters that were available in high resolution for the study area. The land use classification, derived from the 30x30m LANDSAT channels, a terrain model of 30x30m and a model of solar irradiation based on the terrain model were available.

7.2.2 Extended regression model

The parameterization of Scherer assumes, that the Bowen Ratio, i.e., the ratio between sensible and latent heat flux, can be assumed as constant within one vegetation class. This simplifies the real conditions in so far as the Bowen Ratio evidently clusters around a characteristic value for each class, but shows strong dependence on water supply and on interchange resistance. Furthermore, the Bowen Ratio is controlled by parameters like air temperature and water vapor saturation deficit.

As soil moisture controls evapotranspiration by influencing stomata apertures, it has no negligible influence on surface temperature, hence long wave radiation and the Bowen Ratio. Therefore, soil moisture must be considered in modelling energy budget components.

Analyzing the interdependence between the energy budget parameters, it can be shown, that with time- site- and vegetation-specific energy input $E_{S\downarrow}(1-\alpha)+E_{l\downarrow}$, the surface temperature and hence long wave radiation and Bowen ratio in first approximation are controlled only by the interchange resistance dependant on stand geometry, wind velocity and soil moisture (Storl, 1992). Because of this interdependance between soil moisture and surface temperature, a spectral soil moisture index partly explains the variance of long wave emission within the vegetation classes.

Storl (Storl, 1992, 1993, 1994) derived a spectral soil moisture index from TM data for the study area that could be integrated into the regression model and improved significantly variance explanation. The regression equation was therefore written as:

$$E_{l\uparrow} = a\,E_{S\downarrow} + b\,h + c\,SM + \sum_{i=1}^{n} d_i p_i + e \qquad (11)$$

SM ... soil moisture index

The regression coefficients calculated with the image processing module GLOREG (Scherer, 1987, Parlow/Scherer, 1991, Storl 1994) for global multiple linear regression can be interpreted as a measure for the contribution of each data set to the reduction or elevation of long wave radiation and hence surface temperature (Parlow/Scherer, 1991). Therefore, radiance temperatures were transformed to longwave radiation values, using the Stephan-Boltzmann equation:

$$E_{l\uparrow} = \sigma T^4 \qquad (12)$$

Where T is the radiation temperature.

In a further step, long wave radiation with 30x30m resolution was calculated, using the derived regression coefficients and applying equation (11). The radiation temperature was then calculated using the Stephan-Boltzmann-equation (12).

Fig. 1 shows the resolution enhanced radiation temperature of the surface. These thermal data contain information about soil moisture, as far as it influences surface temperature and establish therefore an ideal dataset to model sensible heat flux and evapotranspiration.

7.3 Temperature of free atmosphere

The meteorological situation at the day of satellite overpass was dominated by high pressure conditions with Abisko Station at the center of the high pressure area. Wind velocities ranged between 1,5 and 2,5m/s at Abisko Station at 9h20, the time of satellite overpass. The 10-minute wind measurements clearly show, that the wind direction follows the sun in order to form a well developed local slope/sea wind system perpendicular to the shores of lake Abisko and the southern slopes of Mount Njulla.
The measurements of a radio sonde from Kallax/Lulea, at 100km from the study site were used to interpolate the temperautes of free atmosphere.
The synoptic weather charts show, that Lulea and the study area are under the influence of the same air masses under high pressure. The potential virtual temperatures from the sondage values confirm, that stable atmospheric conditions prevailed, one of the conditions for applying Brehm 's slope wind model.

The uncorrected air pressure, temperature and vapor pressure values of the radio sonde from Lulea, interpolated by the program SONDE (Storl, 1992), showed 967,85 hPa, 12,96 °C and 8,84 hPa respectively for the elevation of Abisko at 385m above sea. The radio sonde started at 12hOO am, whereas the satellite passed at 9h20 am. At Abisko, air temperature rose from 9,13 °C to 10.43 °C in this interval of time, which makes a difference due to time of 1,3 °C. If the temperature measured by the radio sonde at Lulea is reduced by 1,3 ° C, according to the time difference, a hypothetic air temperature at Abisko Station of 11,66 °C at 9h20 is derived. This slightly higher value (2,56 °C) than the temperature of 9,1 °C measured at Abisko station is probably due to the warming effect of the lower landmasses of Lulea and the cooling effect of advected air from Lake Abisko.
It cannot be theoretically justified to simply reduce the temperature profile of the radio sonde by 2,56 °C and adapt it hereby to the measured temperature values at Abisko of 9,1 °C. As air masses at Lulea are warmed up from the underlying land masses, the heating effect is reduced with height, and it can be assumed that the temperature at the upper limit of the mixture layer at 2000-3000m behaves very constant over time and space. Therefore, the radio sonde value for this elevation is taken as a reference in order to model the temperature

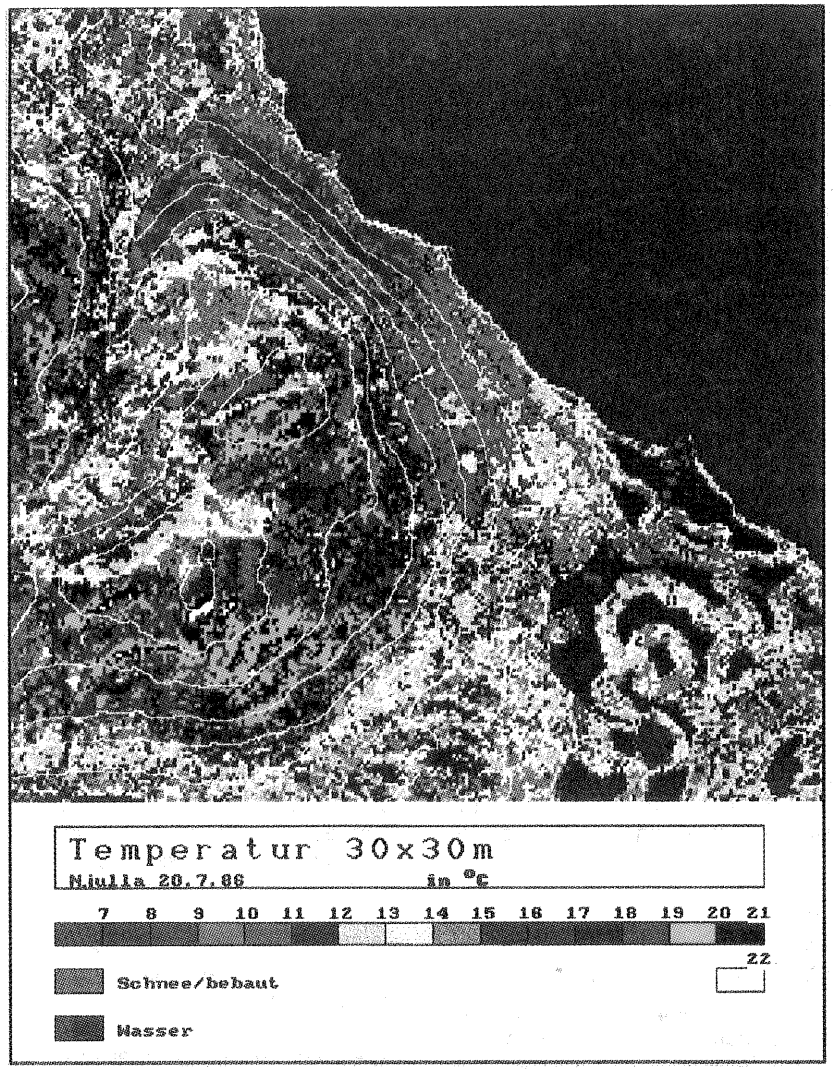

Fig. 1. Surface radiation temperature, resolution enhanced to 30x30m.

gradient between the station values at Abisko and the upper limit of the boundary layer. It is assumed that temperature decreases with elevation in a linear way. This assumption, however, is supported by the linear form of the temperature and vapour pressure curve over Lulea.

Mannstein (Mannstein, 1991) did not consider the modification of air density due to the higher temperature near the surface and the vapor content of the air. The author calculated air density as used in formula (5) from arithmetic means between atmosphere- and surface temperature and the complete formula, considering vapor pressure.

Vapor pressure was modeled in the same way as air temperature, as the profiles showed similar characteristics.

8. SENSIBLE HEAT FLUX MODELLING

The image processing program WAERME (Storl, 1992) developed by the author uses as input four images with the parameters elevation, inclination, land use class, roughness length and surface temperature. Furthermore, a tabular file containing the radio sonde values for air temperature, air- and vapour pressure in an interval of 1m is required.

The program reads for each pixel elevation, inclination, surface temperature, land use class and roughness length and accesses the air temperature, air- and vapour pressure values for the corresponding elevation.

The nucleus of the program calculates potential temperature of air and surface first, so that the difference Δ_s can be derived. The difference Δ between potential surface temperature at the height n+zo and free atmosphere, as required by Brehm's model, is derived by an iterative algorithm. First, the unknown temperature difference Δ is set to 0,5 x Δs (where Δs is the temperature difference between radiance temperature and temperature of free atmosphere). R_o is calculated according to equation (3), and c_g and η are derived from R_o and α, according to the functional dependance between these parameters given by Brehm's results. Δ_d is then calculated by equation (7). If $\Delta_d+\Delta$ is bigger than Δ_s, Δ is reduced by a fraction of itself, and Ro, cg, η and Δd are repeatedly calculated, until equation (8) holds and the difference Δ is known.

The coefficients c_g and η have to be derived for each pixel depending on soil rosby number (as output from the iterative procedure) and slope angle.

Finally, sensible heat flux is calculated by equation (5), and the value is written to an output image.

Fig. 2 shows sensible heat flux, as it was modeled over the study area.

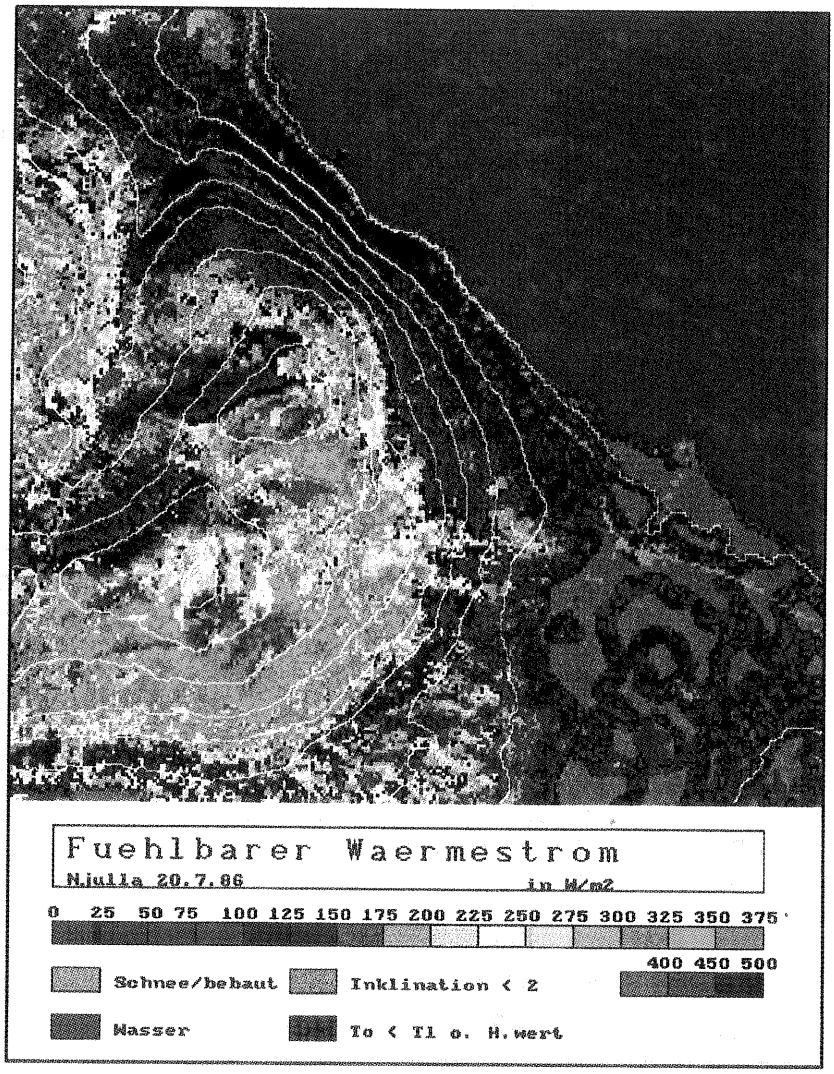

Fig. 2. Sensible heat flux

9. ENERGY BUDGET MODEL

9.1 Soil heat flux

As for the day of satellite overpass no measured data for sensible heat flux were available, verification was performed by integrating the calculated data into an energy budget model.
All energy budget terms of equation (9), except ground heat flux, evapotranspiration and sensible heat flux, were at hand and well determined by ground truth and calibration.
Using a method described by Daughtry, Kustas and Moran (Daughtry/Kustas/Moran, 1990), soil heat flux could easily be derived at pixel resolution and calibrated to the data from Abisko Station (Storl, 1992).
The method applied is described in detail in Storl, 1992.

9.2 Evapotranspiration

The only term left to be calculated is evapotranspiration. This parameter was modeled in a way, that would give good results over specific land use classes as heaths and meadows, for which the assumptions of the applied evaporation model hold. Several authors have shown, that specially in subpolar ecosystems, equilibrium evaporation is a good aproximation to actual evapotranspiration for a wide variety of conditions, counting with sufficient water supply (Davies, 1972, Rouse/Stewart, 1972, Mc Naughton/Black, 1973, Mc Naughton, 1976)
Equilibrium evaporation is written as:

$$Eq = \frac{\Delta}{\Delta + \gamma}(Q^* - G) \qquad (13)$$

Where Δ is the inclination of the saturation curve for vapor pressure, Q^* is the radiation balance, G the ground heat flux and γ the psycrometric constant.

9.3 Ratio H/(Q*-G)

The first condition that has to hold, if the sensible heat flux H is modeled with accuracy, is that the ratio

H/(Q*-G) cannot be grater than 1 and has to show values between 0 and 1.

Fig. 3 shows the image of the ratio H/(Q*-G).

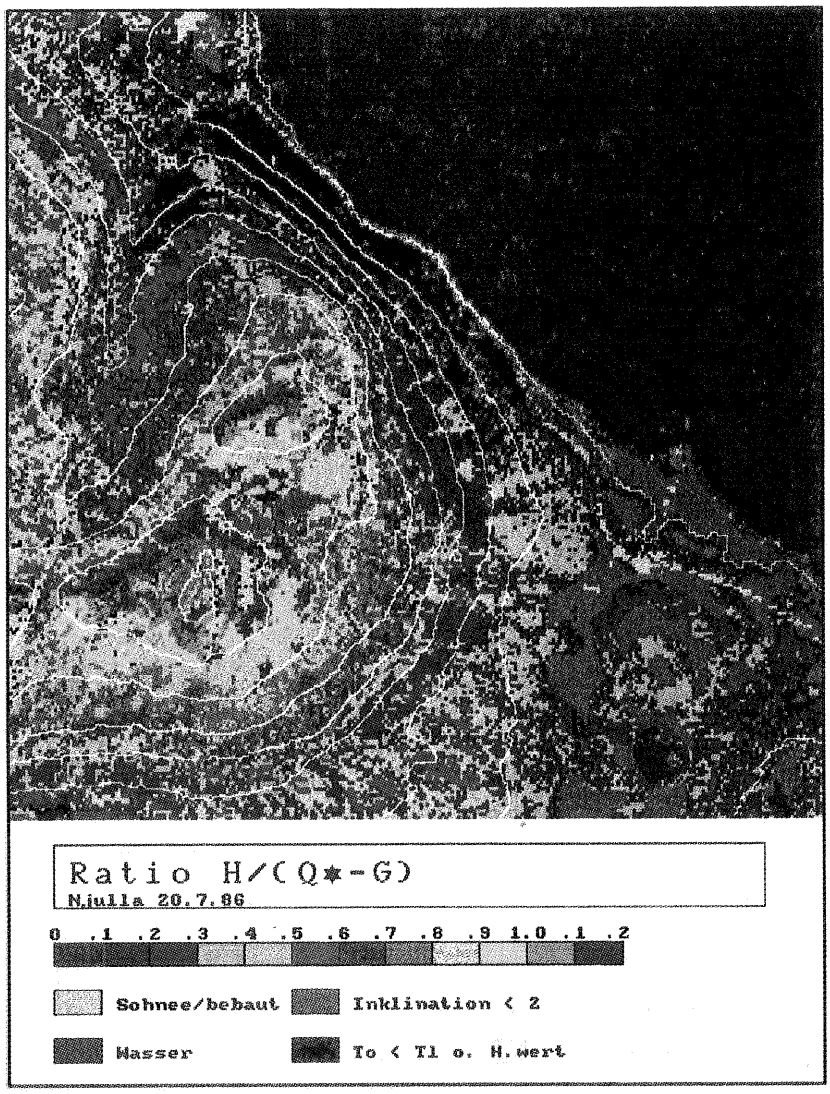

Fig. 3. Ratio H/(Q*-G)

It can be seen, that the ratio value does in no case exceed the value 1,2, and that only for very few pixels the value is greater than 1,0. The high values are limited to the driest and most sunexposed sites (Storl, 1992, 1993, 1994).
As the pixels with values greater than 1.0 are without exception rocky places bare of vegetation, it can be assumed that the ground heat flux has been overestimated in these places. This might be true, as ground heat flux was calculated using the NDVI which shows unproportionally low values for these sites.
It can be shown in detail, how the ratio lowers at all sites that were mapped as moist places in the field campaign (Storl, 1992, 1993, 1994). This has to be so, as soil moisture increases the radiation balance by triggering evopatranspiration. The pattern of the soil moisture index is well defined in the ratio image.

9.4 Ratio (H+LE)/(Q*-G)

The ratio (H+LE)/(Q*-G) theoretically should equal 1,0 in all places, if all energy budget terms were modeled with accuracy.

Fig. 4, showing the ratio image (H+LE)/(Q*-G), can be interpreted in the following way:
The calculated value for Eq must be too high in all cases, where water supply is no longer granted, as the theoretical condition for Eq to be true is unlimited water supply. This condition, at the time of satellite overpass, is surely no longer given on the rocky, sparesly vegetated and sunexposed NE-slopes of mount Njulla. This would explain the values ranging up to 1,7 at these places. In this context, an interesting observation can be made: Looking at the sites that were mapped as moist patches, especially below leaking snow fields, it can be stated, that the values are very close to 1,0. It can be concluded, that the evapotransiration model holds for these sites, as water supply is not limited, and that the model for sensible heat flux produces good values, as the energy budget equation holds. This observation can be made at many representative sites mapped in the field campaign.
All surface types, for which Rouse and Stewart (Rouse/Stewart, 1972) declared equilibrium evaporation to be valid, show values very close to 1,0, as far as they are not obviously subject to water stress.

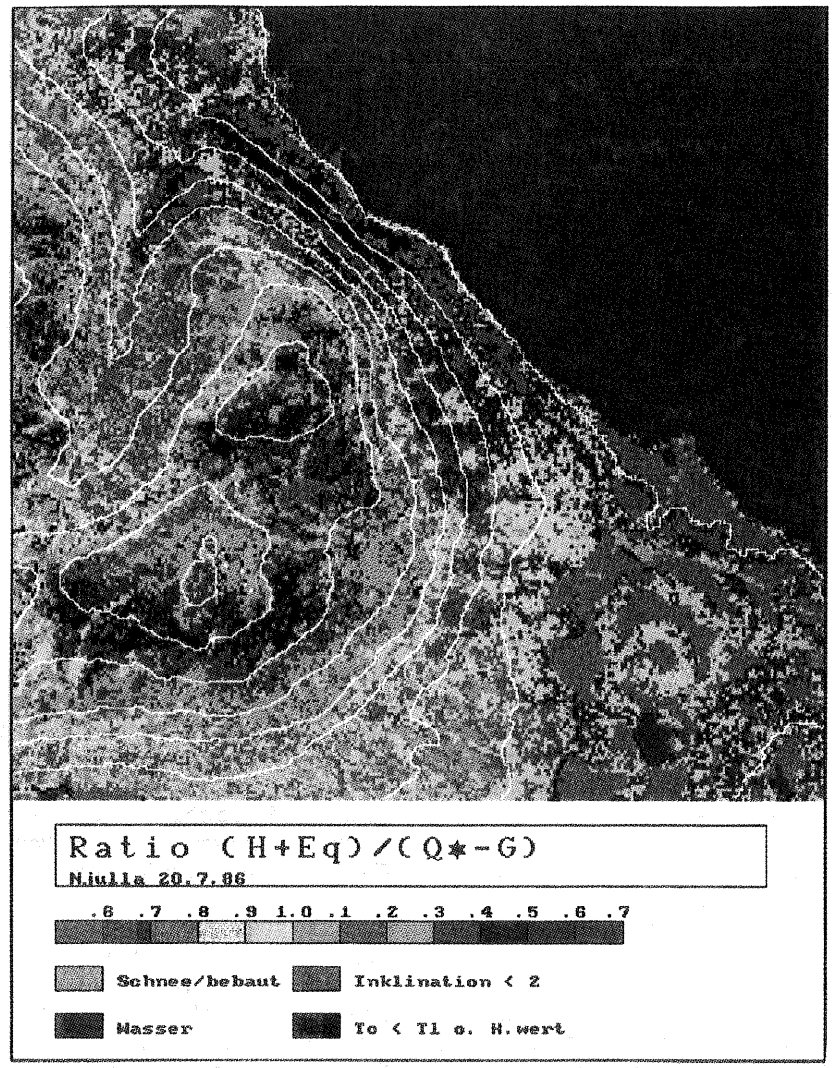

Fig. 4. Ratio (H+LE)/(Q*-G)

Tab. 2 shows the statistics of the ratio (H+LE)/(Q*-G) for some of the land use classes:

very dry heath	dry heath	moist heath	meadow	salix	heath birch forest	moist heath birch forest
1,12	0,84	1,15	1,34	0,93	0,91	0,78

Tab. 2. mean values of (H+LE)/(Q*-G) for different land use classes

The statitics show together with the visual interpretation, that the modelling results have different qualities for the land use classes.
The dry heaths and meadows show values above 1,0. These sites generally show dry conditions, a fact that causes the actual evapotranspiration rate to be lower than the one calculated by Eq. In the case of dry heaths it can be commented, that the land use classification shows a high confusion rate between moist heaths and dry heaths in a way, that many sites that actually are moists heaths are classified as dry heaths. This would explain the low coefficient for dry heaths.
For the heath birch forests, equilibrium evaporation seems to model best the actual evapotranpiration rate. For the moist heath birch forest, this condition is no longer true, as evapotranspiration for this moist forest type evidently is higher than equilibrium evaporation. This observation is supported by the authors who investigated equilibrium evaporation in high latitude sites.(Rouse/Stewart, 1972).

10. CONCLUSIONS

It has been shown, that sensible heat flux can be modeled with good accuracy on mountainous slopes under stable atmospheric conditions, using the slope

wind model of Brehm and the methods suggested in this paper for deriving surface parameters.
It was also shown, that an integration of all energy budget parameters can lead to accurate conclusions about the validity of different models for energy budget parameters under different surface conditions. The energy budget integration is shown to be be an important instrument for the verification of modeled sensible heat flux.

11. REFERENCES

Brehm, M., 1986, Experimentelle und numerische Untersuchungen der Hangwindschicht und ihrer Rolle bei der Erwärmung von Tälern, *Wiss. Mitt. Institute of Meteorology, University of München, pp 54*

Daughtry, C.S.T./Kustas, W.P./Moran, M.S., 1990, Spectral estimation of net radiation and soil heat flux, *Rem. Sens. Env. 32: 111-124*

Davies, J.A., 1972, Actual, potential and equilibrium evaporation for a beanfield in southern Ontario, *Agr. Met., 10: 331-348*

Mannstein, H. , 1991, Die radiometrisch bestimmte Oberflächentemperatur im Gebirge und die Ermittlung des Stroms fühlbarer Wärme, *Deutsche Gesellschaft für Luft- und Raumfahrt, DLR-FB 90-07*

Mc Naughton, K.G./Black, T.A., 1973, A study of evapotranspiration from a douglas fir forest using the energy balance approach. *Water Res. Res., 9: 1579-1590*

Mc Naughton, K.G., 1976, Evaporation and advection II: evaporation downwind of a boundary separating regions having different surface resistances and available energies, *Quart. J. R. Met. Soc., 102: 193-202*

Monin, A.S./Zilitinkevich, S.S., 1968, On description of micro- and mesoscale phenomena in numerical models of the atmosphere, *WMO-IUGG Symp. on Num. Weather Forecast Tokyo, 26.11. - 4.12.1968, Techn. Rep. Japan Meteorol. Agency No. 67, I.105-I.121*

Parlow, E., 1988, Die Ableitung des Strahlungshaushaltes eines subpolaren Ökosystems mit Hilfe der Digitalen Bildverarbeitung, *Habil.-Schrift Geowiss. Fakultät, Univ. Freiburg.*

Parlow, E., 1990, Spatial patterns of radiation fluxes using LANDSAT-TM-data and GIS-techniques, *Proceedings of EARSeL-Symposium at Helsinki,1989, Comm. of Europ. Communities. Brüssel-Luxemburg 1990, pp. 441-447*

Parlow, E./Scherer, D., 1991, Studies of the radiation budget in polar areas using satellite data and GIS-techniques, *IGARSS Helsinki1991, IEEE-Catalog Number 91CH2971-0, Vol. 1, pp. 29-32*

Parlow, E., 1992, Einstrahlungskorrekturen - eine Anwendung für digitale Geländemodelle in der Satellitenfernerkundung, *Freiburger Geographische Hefte, Institute of Physical Geography, University of Freiburg i.Br., Germany, Heft 34, pp. 111-118*

Price, J.C., 1987, Calibration of satellite radiometers and the comparison of vegetation indices., *Rem. Sens. Env., 21: 15-27*

Rouse, W.R., Stewart, R.B., 1972, A simple model for determinig evaporation from high latitude upland sites. *J. Appl. Meteorol., 11: 1063-1070*

Scherer, D. 1987, Die Erfassung subskaliger Strukturen in Oberflächentemperaturbildern mit Hilfe von geographischen Zusatzdaten, *Thesis, Institute of Physical Geography, University of Freiburg i.Br., Germany*

Schott, J.R./Volchok, W.J., 1985, Thematic mapper thermal infrared calibration, *Photogrammetric Engineering and Remote Sensing 51, 9: 1351-1357*

Storl, J., 1992, Methodische Integrierung GIS-gestützter Verfahren zur Verbesserung der flächenhaften Modellierung des Wärmehaushaltes mit LAND-SAT-TM-Daten in Abisko/Schweden, *Thesis, Institute of Geoecology and Meteorology, University of Basel, Suizzerland, Institute of Physical Geography and Hydrology, University of Freiburg i. Br., Germany*

Storl, J., 1993, Ableitung eines hochauflösenden Bodenfeuchte Index aus Landsat-TM Daten, Proceedings of the 12th Scientific Technical Conference of the German Society for Photogrammetry and Remote Sensing DGPF, Augsburg, Germany

Storl, J., 1994, Deriving a high resolution soil moisture index from Landsat-TM data, *VII Symposium of the ISPRS Commission for Resource and Environmental Monitoring, Proceedings, Rio de Janeiro, Brasil, 09/94*